

A Toy Model for the Cycle Rank Dependence of Stretch at Break in Phantom Chain Network Simulations

Yuichi Masubuchi

Department of Materials Physics, Nagoya University, Nagoya 4649603, Japan

mas@mp.pse.nagoya-u.ac.jp

Jan 28, 2026

Submitted to the Journal of Non-Newtonian Fluid Mechanics

Abstract

The relationship between the topological architecture of polymer networks and their macroscopic rupture remains a fundamental challenge in polymer physics. Recent coarse-grained simulations have revealed that the dependence of stretch at break (λ_b) on node functionality and reaction conversion can be unified into a universal master curve when plotted against the cycle rank density (ξ). However, a theoretical derivation explaining this universality has been lacking. This study proposes a simple mechanical model to describe the ξ -dependence of fracture strain. The polymer network is modeled as a mechanical system consisting of a sequence of springs representing localized highly stretched strands and the surrounding unstretched network. By relating the stiffness contrast between these regions to the network connectivity defined by ξ , an analytical expression for the stretch at break is derived: $\lambda_b \propto (2\xi + 5)/(2\xi + 1)$. The proposed model is validated against phantom chain simulations using both Gaussian and finite extensibility (FENE) springs. The theoretical prediction shows excellent agreement with simulation data, providing a physical basis for the phenomenological universality observed in polymer network rupture.

Keywords

polymer networks; coarse-grained models; rupture; fracture; cycle rank

Introduction

The relationship between the topological architecture of polymer networks and their macroscopic mechanical failure remains one of the most fundamental yet elusive challenges in polymer physics.[1] While the linear elasticity of rubberlike materials is well described by classical theories—such as the affine and phantom network models—the mechanisms governing large-

deformation, fracture and rupture are far less well understood. A central difficulty lies in identifying the specific structural descriptors that determine fracture limits, particularly in networks containing topological defects or varying node functionalities.

Historically, theoretical approaches to network fracture have relied heavily on idealized assumptions. The classical Kuhn theory [2,3] estimates the limit of extensibility based solely on the finite extensibility of individual strands, scaling with the square root of the strand degree of polymerization ($N^{1/2}$). Meanwhile, the Lake-Thomas theory [4] connects network structure to fracture energy by assuming that all bonds in a strand must be stressed to rupture. However, these theories often struggle to account for the complex interplay between node functionality (f), reaction conversion (p), and the resulting network connectivity. For instance, the effect of node functionality on strength is contentious; while traditional views suggest higher functionality enhances strength[5], recent experiments on Tetra-PEG gels indicate that lower functionality can yield superior fracture properties under certain conditions [6].

To bridge the gap between molecular topology and macroscopic failure, molecular simulations have become indispensable. As recently reviewed [7], the field has evolved from early studies of crack tips [8,9] to large-scale simulations capable of capturing network heterogeneity [10–14]. Despite persistent challenges regarding mismatches in spatiotemporal scales between simulations and experiments and the validity of coarse-graining in non-equilibrium states, these computational approaches have provided critical insights into how structural defects, such as loops and dangling ends, influence failure.

In a recent series of phantom chain simulations, the rupture of polymer networks formed by end-linking star polymers was systematically investigated [15–22]. By employing a quasi-static energy-minimization approach to eliminate strain-rate artifacts [23–25], the conflicting reports regarding node functionality were resolved. It was demonstrated that the influence of functionality f is highly dependent on the reaction conversion p , specifically, higher f strengthens the network at low conversions, but this trend reverses at high conversions.

Most significantly, these simulations [16–22] revealed that the complex dependencies of fracture stress and strain on f and p can be unified by a single topological parameter: the cycle rank (ξ). The cycle rank represents the density of independent loops within the network and can be calculated via mean-field theories [26,27]. Simulation data for strain λ_b , stress σ_b , and work W_b of rupture were observed to collapse onto universal master curves when plotted against the cycle rank density.

However, while these simulation results establish a strong phenomenological correlation between cycle rank and fracture limits, a theoretical derivation explaining why fracture strain is governed by cycle rank is notably absent. In this paper, a theoretical model is proposed to describe the cycle rank dependence of fracture strain in polymer networks. By reconsidering the distribution of load and network connectivity through the lens of cycle rank, this study aims to provide a physical basis for the universality observed in simulations.

Model

Figure 1 schematically exhibits the model of this study. As seen in the leftmost panel (a), at the network rupture, a highly stretched region is observed, while most of the system remains rather unstretched. Based on this observation, the entire system is replaced by a sequence of three springs with different stiffnesses, k_1 and k_A , as shown in panel (b). Here, $k_1 < k_A$ is assumed that the middle spring is primarily stretched, and rupture occurs when the stretch of the middle spring exceeds a critical value λ_{b1} . For the spring sequence, the spring constant of the entire system k , is written as follows.

$$\frac{1}{k} = \frac{2}{k_A} + \frac{1}{k_1} \quad (1)$$

Concerning the relation between k_1 and k_A , let us consider the configuration in panel (c), which naively represents the boundary between stretched and unstretched regions. Namely, for each node, a single strand in the stretched region (the middle spring) balances the force with the other strands in the unstretched region.

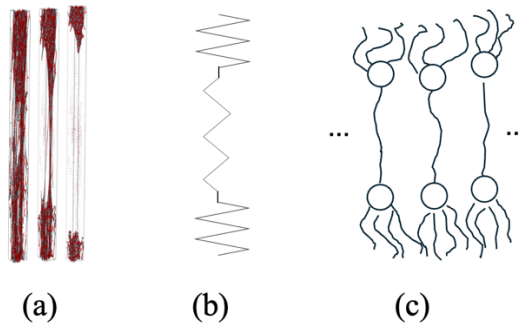


Figure 1 Typical simulation snapshots at the network rupture (a), the sequential 3-spring model, and (c) the naïve strand representation of the 3-spring model.

With the number of contributing strands for single nodes at both ends ν_s , k_A is written as below.

$$k_A = \nu_s k_1 \quad (2)$$

ν_s can be related to the cycle rank ξ , which is defined as follows.

$$\xi = \frac{1}{n_n} (n_{st} - n_n) \quad (3)$$

Here, n_n and n_{st} are the number of effective nodes and strands in the entire system. Given that the number of stretched strands in the middle is $n_n/2$, v_s can be written as follows.

$$v_s = \frac{1}{n_n} \left(n_{st} - \frac{n_n}{2} \right) = \xi + \frac{1}{2} \quad (4)$$

Assuming that the stretch of the middle strand reaches λ_{b1} under a given exerted tension $F_b = k_1 \lambda_{b1}$, the entire stretch λ_b is written as below from eqs 1-5.

$$\lambda_b = \frac{F_b}{k} = \frac{F_b}{k_1} \left(\frac{2}{v_s} + 1 \right) = \lambda_{b1} \left(\frac{2\xi + 5}{2\xi + 1} \right) \quad (5)$$

Here, λ_{b1} is considered as the fitting parameter.

Simulations

The theoretical prediction for λ_b is evaluated by comparing it with phantom network simulations. Since the simulation data have already been published separately [15–22], a brief explanation of the simulation is given here. Rouse-Ham-type star-branched prepolymers with f branching arms, each consisting of N_a beads connected by linear springs, are dispersed in a simulation box with periodic boundary conditions. Units of length, energy, and time are chosen as the equilibrium bond length a , the thermal energy $k_B T$, and the bead diffusion time $\tau = \zeta a^2/k_B T$, where ζ is the friction coefficient of the single bead. The bead number density is fixed at 8, and the number of branching arms in the system is ca. 3300. After the system equilibrates, the end-linking reactions are turned on. The reaction occurs only between different prepolymers to prevent the formation of primary loops, as in the experimental setup for PEG gels [28]. In the resultant networks, the spring number per strand is $N_s = 2N_a + 1$. The simulation snapshots are stored at designated conversion p , ranging from 0.6 to 0.95. The stored networks are repeatedly subjected to a set of energy-minimization and infinitesimal stepwise deformations. During this elongation, bonds are removed when their length exceeds a designated critical length b_c . The total energy for the Gaussian network case is as follows.

$$U = \frac{3k_B T}{2a^2} \sum_{i,j} \mathbf{b}_{ij}^2 \quad (6)$$

Here, \mathbf{b}_{ik} is the bond vector between beads i and j . For this case, b_c was chosen at $\sqrt{1.5}$. For comparison, FENE networks are also examined with the total energy given below.

$$U = -\frac{3k_B T b_{\max}^2}{2a^2} \sum_{i,k} \ln \left(1 - \frac{\mathbf{b}_{ik}^2}{b_{\max}^2} \right) \quad (7)$$

Here, b_{\max} is a nonlinear parameter set to 2, and b_c was chosen to be $\sqrt{3.6}$. The stretch at break, λ_b , is determined from the peak of the nominal stress-strain curve. For statistics, eight

independent simulations are performed for each condition.

Results and Discussion

Figure 2 compares eq 5 with the previous simulation results for various strand molecular weights [21]. By varying the parameter λ_{b1} , eq 5 agrees with the data within the error bars.

The presented ξ -dependence of λ_b has been described by a power law as $\lambda_b \propto \xi^{-\alpha}$ [16–22,29]. However, such a description is unphysical in the limit of $\xi \rightarrow \infty$, where λ_b diminishes to zero. For well-developed networks with large ξ , λ_b is expected to approach a certain value rather than zero. Eq 5 is consistent with this expectation, although in the examined range of ξ , such a behavior is not observed.

In the limit of $\xi \rightarrow 0$, eq 5 suggests a constant value. The data are inconsistent with this prediction, as they show a power-law-like increase. This discrepancy arises because, with a small value of ξ , the model setting shown in Fig 1 is incorrect. Namely, the theory assumes only one single strand is stretched, whereas in this ξ range, a couple of single strands are sequentially connected and stretched to realize large λ_b values. Indeed, the data at $\xi \sim 0.02$ correspond to $f = 3$ and $p = 0.6$, which yield fewer than 2 arms per branch point reacted.

To take into account such an effect, eq 1 should be modified as

$$\frac{1}{k} = \frac{2}{k_A} + \frac{N_1(\xi)}{k_1} \quad (8)$$

Here, $N_1(\xi)$ is the number of stretched strands dependent on ξ . N_1 is probably related to the number of strand-extending prepolymers discussed previously[15,16]. Nevertheless, for simplicity, this study employs $N_1 = 1$, given that eq 5 reasonably reproduces the data in most of the examined range of ξ . The other reason for the discrepancy in the small- ξ range is that the theory does not account for nonlinearity, which arises even under large deformations in networks of linear springs.

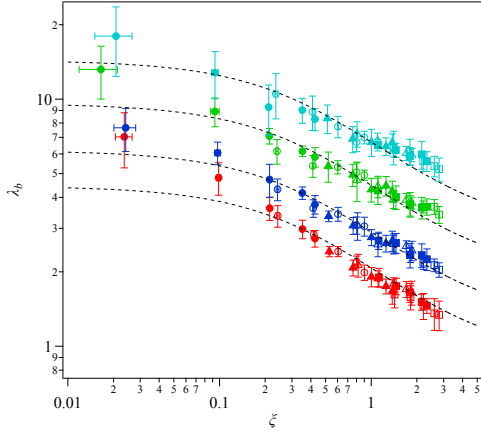


Figure 2 Comparison of the theory (eq 5) with the simulation results for Gaussian spring networks [21] with the strand length at 7 (red), 11 (blue), 21 (green), and 41 (sky blue). Symbols indicate $f = 3$ (filled circle), 4 (unfilled circle), 5 (filled triangle), 6 (unfilled triangle), 7 (filled square), and 8 (unfilled square). Error bars correspond to the standard deviations for eight different simulation runs for each condition. Broken curves show eq 5.

Although the basic setting differs from the theoretical model, eq 6 is compared with simulation results using FENE springs [22] in Fig 4. The other parameters are the same as those for the Gaussian networks, except for the bond-breaking parameter b_c , which was $\sqrt{1.5}$ for the Gaussian networks and $\sqrt{3.6}$ for the FENE networks, as mentioned above. The results are essentially the same as those shown in Fig 2, demonstrating that the proposed equation reasonably describes the data for $\xi \gtrsim 0.02$.

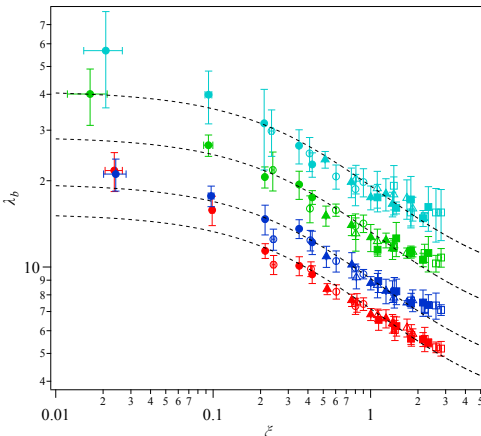


Figure 3 Comparison of the theory (eq 5) with the simulation results for FENE spring networks [22] with the strand length at 7 (red), 11 (blue), 21 (green), and 41 (sky blue). Symbols indicate $f = 3$ (filled circle), 4 (unfilled circle), 5 (filled triangle), 6 (unfilled triangle), 7 (filled square), and 8 (unfilled square). Error bars correspond to the standard deviations for eight different simulation runs for each condition.

8 (unfilled square). Error bars correspond to the standard deviations for eight different simulation runs for each condition. Broken curves show eq 5.

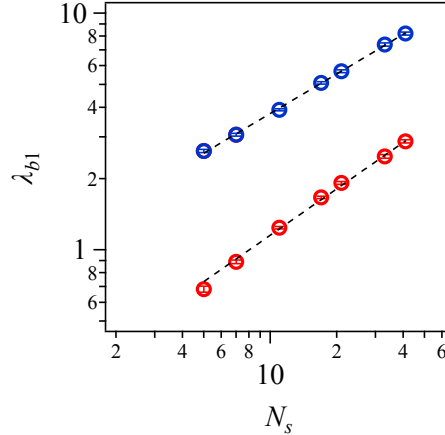


Figure 4 λ_{b1} obtained from the fitting shown in Figs 2 and 3 plotted against N_s . Red and blue symbols show the cases for Figs 2 (Gaussian springs) and 3 (FENE springs), respectively.

From the fitting in Figs 2 and 3, the value of λ_{b1} is extracted and plotted against the strand molecular weight N_s in Fig 4. The dotted lines show a power-law fit. The exponents are 0.66 and 0.55 for the Gaussian and FENE spring networks. The difference in the absolute value is due to the chosen bond-breaking parameter. According to the crude model in Fig. 1, the exponent is expected to be 0.5, but the observed values are higher, suggesting that the force balance in the simulated networks is more complex. Nonetheless, the result in Fig 4 is consistent with earlier studies that approximated $\lambda_b(\xi)$ as a power-law function [21,22].

One may argue that the proposed theory must be tested against experimental data, not only against specific simulations. Such an attempt is shown in Fig 5, where the experimental result for a double network gel is compared with eq 5. In the experiment [30], yielding in the stress-strain curve, induced by the breakage of the PEG network, was observed while the PAMPS network was maintained. The vertical axis shows the yield strain λ_y divided by the swelling ratio λ_s . The cycle rank was estimated using mean-field theory based on the experimental settings for f and p . The theoretical curve attains reasonable agreement with $\lambda_{b1} = 5.8$. Although there have been lots of experimental reports on the toughness of network polymers, datasets with specified f and p are rather rare.

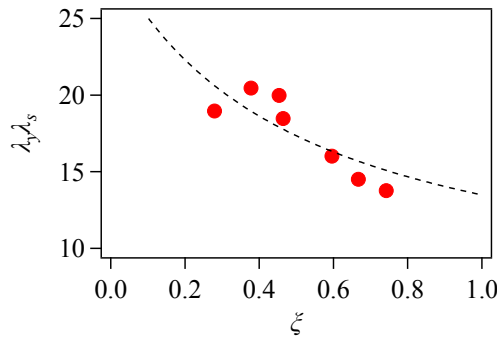


Figure 5 Comparison of the theory (eq 5) with the experimental result for PAMPS-PEG double network gels [30] shown by symbols. The broken curve shows eq 5 with $\lambda_{b1} = 5.8$.

Concluding remarks

According to the crude mechanical model, the ξ -dependence of λ_b for phantom chain networks was derived as $\lambda_b = \lambda_{b1} (2\xi + 5)/(2\xi + 1)$, where λ_{b1} is the fitting parameter. The proposed equation was tested against reported simulation results for Gaussian and FENE spring networks, demonstrating reasonable agreement for $\xi \gtrsim 0.2$. λ_{b1} depended on the strand molecular weight N_s with a power-law relation. The exponent was slightly larger than 0.5, being consistent with previous reports that empirically expressed the ξ -dependence of λ_b as power-law functions. The theory was also tested against experimental data for double network gels, yielding reasonable agreement.

Although the proposed function is promising for further testing through experiments and simulations, the proposed theory addresses λ_b only and does not describe stress at break or work of fracture, as this study constructed a one-dimensional mechanical model that did not account for strand density and connectivity. The N_s -dependence of λ_{b1} shown in Fig 4 also implies the necessity of further consideration of this parameter. Subsequent studies in such directions are ongoing, and the results will be reported elsewhere.

Acknowledgements

This study was partly supported by the Hibi Foundation.

References

- [1] Takamasa. Sakai, Physics of Polymer Gels, Wiley, 2020.
<https://doi.org/10.1002/9783527346547>.
- [2] W. Kuhn, Dependence of the average transversal on the longitudinal dimensions of

statistical coils formed by chain molecules, *Journal of Polymer Science* 1 (1946) 380–388. <https://doi.org/10.1002/pol.1946.120010505>.

[3] S.P. Obukhov, M. Rubinstein, R.H. Colby, *Network Modulus and Superelasticity*, 1994. <https://pubs.acs.org/sharingguidelines>.

[4] J. Lake, A.G. Thomas, The strength of highly elastic materials, *Proc. R. Soc. Lond. A Math. Phys. Sci.* 300 (1967) 108–119. <https://doi.org/10.1098/rspa.1967.0160>.

[5] J. Fu, Strong and tough hydrogels crosslinked by multi-functional polymer colloids, *J. Polym. Sci. B Polym. Phys.* 56 (2018) 1336–1350. <https://doi.org/10.1002/polb.24728>.

[6] T. Fujiyabu, N. Sakumichi, T. Katashima, C. Liu, K. Mayumi, U. Chung, T. Sakai, Tri-branched gels: Rubbery materials with the lowest branching factor approach the ideal elastic limit, *Sci. Adv.* 8 (2022) abk0010_1-abk0010_10. <https://doi.org/10.1126/sciadv.abk0010>.

[7] Y. Masubuchi, T. Ishida, Y. Koide, T. Uneyama, A review on molecular simulations for the rupture of cross-linked polymer networks, *Sci. Technol. Adv. Mater.* 26 (2025). <https://doi.org/10.1080/14686996.2025.2587391>.

[8] M.J. Stevens, Manipulating connectivity to control fracture in network polymer adhesives, *Macromolecules* 34 (2001) 1411–1415. <https://doi.org/10.1021/ma0009505>.

[9] M.J. Stevens, Interfacial Fracture between Highly Cross-Linked Polymer Networks and a Solid Surface: Effect of Interfacial Bond Density, *Macromolecules* 34 (2001) 2710–2718. <https://doi.org/10.1021/ma000553u>.

[10] C.W. Barney, Z. Ye, I. Sacligil, K.R. McLeod, H. Zhang, G.N. Tew, R.A. Riddleman, A.J. Crosby, Fracture of model end-linked networks, *Proceedings of the National Academy of Sciences* 119 (2022) 2–7. <https://doi.org/10.1073/pnas.2112389119>.

[11] K. Hagita, T. Murashima, Critical Importance of Both Bond Breakage and Network Heterogeneity in Hysteresis Loop on Stress–Strain Curves and Scattering Patterns, *Macromolecules* 57 (2024) 10903–10911. <https://doi.org/10.1021/acs.macromol.4c01996>.

[12] T. Furuya, T. Koga, Molecular Simulation of Effects of Network Structure on Fracture Behavior of Gels Synthesized by Radical Polymerization, *Macromolecules* 58 (2025) 3359–3368. <https://doi.org/10.1021/acs.macromol.4c02875>.

[13] Y. Higuchi, K. Saito, T. Sakai, J.P. Gong, M. Kubo, Fracture Process of Double-Network Gels by Coarse-Grained Molecular Dynamics Simulation, *Macromolecules* 51 (2018) 3075–3087. <https://doi.org/10.1021/acs.macromol.8b00124>.

[14] S. Uehara, Y. Wang, Y. Ootani, N. Ozawa, M. Kubo, Molecular-Level Elucidation of a Fracture Process in Slide-Ring Gels via Coarse-Grained Molecular Dynamics Simulations, *Macromolecules* 55 (2022) 1946–1956.

https://doi.org/10.1021/acs.macromol.1c01981.

[15] Y. Masubuchi, Y. Doi, T. Ishida, N. Sakumichi, T. Sakai, K. Mayumi, T. Uneyama, Phantom Chain Simulations for the Fracture of Energy-Minimized Tetra- and Tri-Branched Networks, *Macromolecules* 56 (2023) 2217–2223.
https://doi.org/10.1021/acs.macromol.3c00047.

[16] Y. Masubuchi, Y. Doi, T. Ishida, N. Sakumichi, T. Sakai, K. Mayumi, K. Satoh, T. Uneyama, Phantom-Chain Simulations for the Effect of Node Functionality on the Fracture of Star-Polymer Networks, *Macromolecules* 56 (2023) 9359–9367.
https://doi.org/10.1021/acs.macromol.3c01291.

[17] Y. Masubuchi, Phantom Chain Simulations for the Effect of Stoichiometry on the Fracture of Star-Polymer Networks, *Nihon Reoroji Gakkaishi* 52 (2024) 21–26.
https://doi.org/10.1678/rheology.52.21.

[18] Y. Masubuchi, Phantom chain simulations for fracture of end-linking networks, *Polymer (Guildf)*. 297 (2024) 126880. https://doi.org/10.1016/j.polymer.2024.126880.

[19] Y. Masubuchi, Phantom chain simulations for fracture of polymer networks created from star polymer mixtures of different functionalities, *Polym. J.* 56 (2024) 163–171.
https://doi.org/10.1038/s41428-023-00862-w.

[20] Y. Masubuchi, T. Ishida, Y. Koide, T. Uneyama, Phantom chain simulations for the fracture of star polymer networks with various strand densities, *Soft Matter* 20 (2024) 7103–7110. https://doi.org/10.1039/D4SM00726C.

[21] Y. Masubuchi, Phantom Chain Simulations for the Fracture of Star Polymer Networks on the Effect of Arm Molecular Weight, *Macromolecules* 58 (2025) 6399–6405.
https://doi.org/10.1021/acs.macromol.5c00475.

[22] Y. Masubuchi, T. Ishida, Y. Koide, T. Uneyama, Influence of Stretching Boundary Conditions on Fracture in Phantom Star Polymer Networks: From Volume to Cross-sectional Area Conservation, (2025). https://doi.org/10.48550/arXiv.2509.01844.

[23] A. Arora, T.S. Lin, B.D. Olsen, Coarse-Grained Simulations for Fracture of Polymer Networks: Stress Versus Topological Inhomogeneities, *Macromolecules* 55 (2022) 4–14.
https://doi.org/10.1021/acs.macromol.1c01689.

[24] K. Nishi, M. Chijiishi, Y. Katsumoto, T. Nakao, K. Fujii, U. Chung, H. Noguchi, T. Sakai, M. Shibayama, Rubber elasticity for incomplete polymer networks, *J. Chem. Phys.* 137 (2012) 224903. https://doi.org/10.1063/1.4769829.

[25] M. Lang, Elasticity of Phantom Model Networks with Cyclic Defects, *ACS Macro Lett.* 7 (2018) 536–539. https://doi.org/10.1021/acsmacrolett.8b00020.

[26] C.W. Macosko, D.R. Miller, A New Derivation of Average Molecular Weights of Nonlinear Polymers, *Macromolecules* 9 (1976) 199–206.

<https://doi.org/10.1021/ma60050a003>.

- [27] D.R. Miller, C.W. Macosko, A New Derivation of Post Gel Properties of Network Polymers, *Macromolecules* 9 (1976) 206–211. <https://doi.org/10.1021/ma60050a004>.
- [28] T. Sakai, Gelation mechanism and mechanical properties of Tetra-PEG gel, *React. Funct. Polym.* 73 (2013) 898–903. <https://doi.org/10.1016/j.reactfunctpolym.2013.03.015>.
- [29] Y. Masubuchi, Y. Koide, T. Ishida, T. Uneyama, Brownian simulations for fracture of star polymer phantom networks, *Polym. J.* 57 (2025) 483–489. <https://doi.org/10.1038/s41428-024-00992-9>.
- [30] T. Matsuda, N. Kashimura, T. Sakai, T. Nakajima, T. Matsushita, J.P. Gong, Yielding of Double-Network Hydrogels with Systematically Controlled Tetra-PEG First Networks, *Macromolecules* 58 (2025) 6017–6032. <https://doi.org/10.1021/acs.macromol.4c02446>.